Nerandomilast (BI 1015550) attenuating pulmonary fibrosis in a mouse model of rheumatoid arthritis-associated interstitial lung disease by modulating the TGF-β1/PI3K/Akt signaling pathway

Xiaohong Wang[1,2], Xi Liu[1,3], Xue Zhong[1,4], Lin Tang[1]

[1]Department of Rheumatology and Immunology, The Second Affiliated Hospital of Chongqing Medical University, Chongqing, China; [2]Department of Geriatrics, Chongqing General Hospital, Chongqing University, Chongqing, China; [3]Department of Geriatrics, Chongqing Medical University, Chongqing, China; [4]Neuro Immune Connections & Repair Lab, Department of Immunology and Infection, Biomedical Research Institute, Hasselt University, Diepenbeek, Belgium

Contributions: (I) Conception and design: X Wang, X Liu, L Tang; (II) Administrative support: X Zhong, L Tang; (III) Provision of study materials or patients: X Zhong, L Tang; (IV) Collection and assembly of data: X Wang; (V) Data analysis and interpretation: X Wang, X Liu; (VI) Manuscript writing: All authors; (VII) Final approval of manuscript: All authors.

Correspondence to: Lin Tang, PhD. Department of Rheumatology and Immunology, The Second Affiliated Hospital of Chongqing Medical University, No. 74, Linjiang Road, Yuzhong District, Chongqing 400010, China. Email: hopetang@hospital.cqmu.edu.cn.

Background: Rheumatoid arthritis-associated interstitial lung disease (RA-ILD) is a severe extra-articular manifestation of rheumatoid arthritis, leading to increased mortality and impaired quality of life. However, effective therapeutic strategies remain limited, highlighting the need to explore novel treatments for RA-ILD. This study aimed to evaluate the ability of nerandomilast (BI 1015550) to attenuate joint inflammation and pulmonary fibrosis in a murine model of RA-ILD, with particular emphasis on the potential involvement of the transforming growth factor-β1 (TGF-β1)/phosphoinositide 3-kinase (PI3K)/protein kinase B (Akt) signaling pathway in mediating its antifibrotic effects.

Methods: A total of 20 male DBA/1 mice (a classic collagen-induced arthritis-susceptible strain) aged 8 weeks were randomly assigned to four groups: control (n=3), RA-ILD (n=5), nerandomilast (BI 1015550) (n=6), and nintedanib (n=6). RA-ILD was induced in all mice except those in the control group using bovine type II collagen (bCII). Nerandomilast and nintedanib were orally administered to the respective treatment groups on alternate days for 12 weeks. Serum tumor necrosis factor-alpha (TNF-α) levels were measured using enzyme-linked immunosorbent assay (ELISA), while immunohistochemistry was performed to evaluate TNF-α and matrix metalloproteinase-3 (MMP3) expression in knee joint tissues. In addition, the expression levels of Col-IV, fibronectin, MMP3, TNF-α, TGF-β1, total and phosphorylated PI3K, and total and phosphorylated Akt in lung tissues were quantified by Western blot analysis.

Results: Nerandomilast significantly reduced serum TNF-α levels in RA-ILD mice ($P<0.05$). Treatment with nerandomilast alleviated pulmonary inflammatory cell infiltration and collagen deposition, while significantly reducing alveolar inflammation and Ashcroft scores ($P<0.05$). Compared with the RA-ILD group, the nerandomilast-treated group exhibited markedly lower protein expression levels of Col-IV, fibronectin, MMP3, TGF-β1, and TNF-α in lung tissues ($P<0.05$). Furthermore, the nerandomilast group showed significantly decreased p-PI3K/PI3K and p-Akt/Akt expression ratios compared with the RA-ILD group ($P<0.05$).

Conclusions: Nerandomilast exerts significant protective effects against pulmonary inflammation and fibrosis in RA-ILD mice, potentially through the downregulation of TNF-α expression and modulation of the TGF-β1/PI3K/Akt signaling pathway.

Keywords: Nerandomilast (BI 1015550); rheumatoid arthritis (RA); interstitial lung disease (ILD); transforming growth factor-β1 (TGF-β1); phosphoinositide 3-kinase/protein kinase B (PI3K/Akt)

Submitted Apr 26, 2026. Accepted for publication Jul 01, 2026. Published online Jul 17, 2026.
doi: 10.21037/jtd-2026-1131
View this article at: https://dx.doi.org/10.21037/jtd-2026-1131

Introduction

Rheumatoid arthritis (RA) is a chronic autoimmune disease characterized by synovial inflammation, synoviocyte hyperplasia, bone and cartilage destruction, and progressive joint deformity (1). RA has a relatively high global prevalence, affecting approximately 0.25–1% of the population (2). Extra-articular manifestations are common in RA, among which interstitial lung disease (ILD) is the most prevalent, with an estimated prevalence of approximately 18.7%. Patients with RA-associated ILD (RA-ILD) exhibit a mortality rate nearly three times higher than that of patients with RA alone (3,4), with a median survival ranging from 2 to 14 years (5). In addition to its high mortality, RA-ILD is associated with substantial functional impairment, diminished quality of life, and increased healthcare burden (6). Although glucocorticoids, immunosuppressive agents, and antifibrotic therapies are widely used in clinical practice, a standardized therapeutic strategy for RA-ILD is yet to be established (7).

The pathogenesis of RA-ILD is multifactorial and involves genetic susceptibility, environmental factors, immune dysregulation, and chronic inflammation (8). Activation of fibroblasts and their subsequent differentiation into myofibroblasts promote the synthesis and deposition of extracellular matrix (ECM) components, while also enhancing matrix metalloproteinase (MMP) activity, ultimately contributing to the progression of pulmonary fibrosis (9,10). Tumor necrosis factor-alpha (TNF-α), a pro-inflammatory and pro-fibrotic cytokine, induces the expression of transforming growth factor-beta (TGF-β), thereby promoting fibroblast proliferation (11). Persistent activation of TGF-β is considered a key mechanism underlying fibroblast activation and fibrotic remodeling (12). Although the pro-fibrotic role of the transforming growth factor-β (TGF-β)/Smad signaling pathway has been extensively investigated, increasing evidence has demonstrated that non-Smad signaling pathways, particularly the phosphoinositide 3-kinase (PI3K)/protein kinase B (Akt) pathway, also play synergistic roles in the pathogenesis of pulmonary fibrosis (13). The PI3K/Akt signaling pathway regulates cell survival, proliferation, and differentiation and is critically involved in numerous physiological and pathological processes (14,15). Furthermore, aberrant activation of the PI3K/Akt pathway has been shown to accelerate ILD progression (16), suggesting that inhibition of this pathway may represent a promising therapeutic strategy for pulmonary fibrosis.

Phosphodiesterase 4 (PDE4) hydrolyzes cyclic adenosine monophosphate (cAMP) and is implicated in regulating various pathophysiological processes including cell proliferation, differentiation, and inflammation (17). PDE4 is highly expressed in immune and inflammatory cells associated with pulmonary inflammatory diseases (18). Previous studies have revealed the significant anti-inflammatory and antifibrotic effects of PDE4 inhibitors (19-22). Nerandomilast (BI 1015550) is a novel PDE4 inhibitor that has been shown to suppress TGF-β1-induced transdifferentiation of lung fibroblasts into myofibroblasts while reducing ECM protein expression (23). Concurrently, it also improves forced vital capacity (FVC) while attenuating bleomycin-induced pulmonary fibrosis in mouse models (23). Owing to its dual anti-inflammatory and antifibrotic activities, nerandomilast has been positioned as a promising therapeutic candidate for ILD (18,23). In

Highlight box

Key findings

- Nerandomilast (BI 1015550) reduced pulmonary inflammation and fibrosis in a murine model of rheumatoid arthritis-associated interstitial lung disease (RA-ILD), as shown by decreased histopathological injury, collagen deposition, and profibrotic signaling activity.

What is known and what is new?

- RA-ILD is a severe extra-articular complication of rheumatoid arthritis with limited treatment options. Although PDE4B inhibition is linked to inflammatory regulation, its role in RA-ILD is unclear.
- This study shows that nerandomilast (BI 1015550) has anti-inflammatory and anti-fibrotic effects in RA-ILD and is associated with inhibition of the transforming growth factor-β1/phosphoinositide 3-kinase/protein kinase B pathway.

What is the implication, and what should change now?

- Targeting PDE4B may offer a disease-modifying strategy for RA-ILD. Nerandomilast (BI 1015550) warrants further translational and clinical evaluation in fibrotic interstitial lung diseases.

addition, apremilast, another PDE4 inhibitor, has been reported to ameliorate autoimmune uveitis in mice by inhibiting the PI3K/Akt signaling pathway (24). However, whether nerandomilast alleviates pulmonary fibrosis in RA-ILD through the TGF-β1/PI3K/Akt signaling pathway remains to be further clarified. Thus, using bovine type II collagen (bCII), an RA-ILD mouse model was hereby established in male DBA/1 mice to investigate whether nerandomilast mitigates pulmonary fibrosis through inhibition of the TGF-β1/PI3K/Akt pathway. We present this article in accordance with the ARRIVE reporting checklist (available at https://jtd.amegroups.com/article/view/10.21037/jtd-2026-1131/rc).

Methods

Experimental animals

A total of 20 male DBA/1 mice (8 weeks old, 18–25 g) were sourced from Beijing Charles River Co., Ltd. Animal License Number: SYXK (Yu) 2023-0005. Mice were kept under standardized housing conditions (22±2 ℃, 12 h light/dark cycle), with free access to food and water. All animals were acclimatized to the rearing environment for 7 days prior to the experiment. All animal experiments were performed under a project license (No. IAC-B2019011-P-01) granted by the Ethics Committee of Greentech, in compliance with institutional guidelines for the care and use of animals.

Materials

Nerandomilast (BI 1015550) and nintedanib were purchased from Adooq Bioscience (Boston, MA, USA), both dissolved in 0.5% carboxymethylcellulose sodium (CMCNa) for suspension preparation. Primary antibodies against TGF-β1 (Cat. No. AF1027), collagen IV (Col-IV; Cat. No. AF0510), phosphorylated Akt (p-Akt; Cat. No. AF0016), and total Akt (Cat. No. AF6261) were obtained from Affinity Biosciences (Cincinnati, OH, USA). Antibodies targeting TNF-α (Cat. No. 26162-1-AP), fibronectin (Cat. No. 15613-1-AP), and glyceraldehyde-3-phosphate dehydrogenase (GAPDH) (Cat. No. 10494-1-AP) were from Proteintech (Wuhan, China), while TNF-α (Cat. No. GB115702) and MMP3 (Cat. No. GB11131) antibodies were acquired from Servicebio (Wuhan, China). Besides, antibodies against phosphorylated PI3K (p-PI3K; Cat. No. 4228) and total PI3K (Cat. No. 4257) were acquired from Cell Signaling Technology (CST; Danvers, MA, USA). The horseradish peroxidase (HRP)-conjugated goat anti-rabbit IgG secondary antibody (Cat. No. 021042) was purchased from EarthOx (Millbrae, CA, USA).

Animal grouping and model establishment

A total of 20 male DBA/1 mice were used in this study. The DBA/1 mouse strain is widely used to establish the collagen-induced arthritis (CIA) model. Among them, 3 served as controls, while the remaining 17 were employed to establish the RA-ILD model. Model mice received initial immunization via subcutaneous multipoint injection at the tail base. Each mouse was injected with 100 μL emulsion, which was prepared on ice by mixing equal volumes of complete Freund's adjuvant (CFA) and bCII (2 mg/mL). The initial injection day was designated as Week 0 (0 w). Three weeks later, a booster injection was administered using an emulsion prepared on ice with equal volumes of incomplete Freund's adjuvant (IFA) and bCII, applied at the identical dosage and injection sites. Following immunization, all 17 mice developed varying degrees of joint swelling and erythema. According to comparable mean arthritis scores, these 17 model mice were allocated into the following three groups: the RA-ILD group (n=5), the nerandomilast (BI 1015550) group (n=6), and the nintedanib group (n=6). Following that, nerandomilast (BI 1015550) (12.5 mg/kg) and nintedanib (100 mg/kg) were administered to the respective treatment groups via oral gavage every other day for 12 weeks, whereas the control and RA-ILD groups received an equivalent volume of 0.5% CMCNa. At Week 19, all mice were anesthetized with propofol and euthanized, and their tissues were collected for subsequent analyses. *Figure 1* presents the detailed schedule of model induction, drug administration, and sample collection.

Sample collection and storage

Upon anesthesia, blood samples were collected via orbital puncture to determine TNF-α levels. The right lung tissues were promptly snap-frozen and stored at −80 ℃ for subsequent Western blot analysis. The left lungs were excised for histological evaluation using hematoxylin and eosin (H&E) staining and Masson's trichrome staining, whereas right knee joints were collected and processed for H&E staining and immunohistochemical analysis.

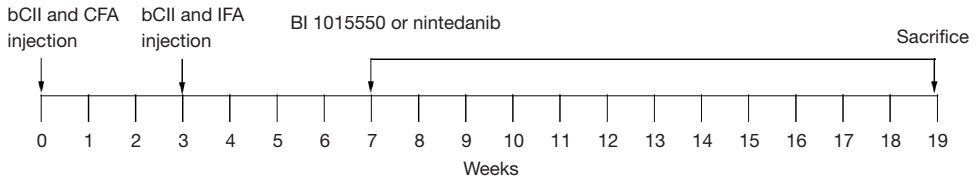

Figure 1 Schematic representation of RA-ILD model induction and subsequent drug treatment. bCII, bovine type II collagen; CFA, complete Freund's adjuvant; RA-ILD, rheumatoid arthritis-associated interstitial lung disease.

Body weight measurement and arthritis scoring

Body weight and visual arthritis scores of the mice were documented weekly from modeling initiation to euthanasia (25). Joint inflammation was assessed and scored by three independent observers blinded to the experimental grouping.

Enzyme-linked immunosorbent assay (ELISA)

Serum TNF-α concentrations were quantified using a commercially available Mouse TNF-α ELISA kit (Multi Sciences Biotech Co., Ltd., Hangzhou, China; Cat. No. EK282) following the manufacturer's protocol. Standards and serum samples (5 μL/well) were incubated with a biotin-conjugate solution (50 μL/well) in antibody-precoated plates for 2 h at room temperature (25±3 ℃) on a shaker (100–300 rpm). After washing, streptavidin-HRP was added and incubated for 45 min protected from light. Following color development with 3,3',5,5'-tetramethylbenzidine (TMB) substrate and subsequent reaction termination, absorbance was measured at 450 nm with reference correction at 570 nm. Absolute TNF-α concentrations were calculated based on the standard curve.

Pulmonary and joint histopathology

Left lung tissues were collected, fixed in an appropriate fixative, embedded in paraffin, and sectioned for histological analysis. Sections were subjected to H&E staining for assessing tissue morphological features and Masson's trichrome staining to evaluate collagen deposition. Alveolar inflammation was quantified using the Szapiel scoring method (25), and pulmonary fibrosis was evaluated according to the modified Ashcroft scoring system (26). Besides, right knee joints were carefully excised, and the surrounding muscle tissue was removed, followed by fixation, decalcification, paraffin embedding, and sectioning. Moreover, synovitis was assessed on H&E-stained sections, whereas cartilage damage was assessed on Safranin O-Fast Green-stained sections (27). Immunohistochemical staining was further conducted to assess the expression levels of TNF-α and MMP3 in the right knee joints. For each sample, three representative images were randomly captured using CaseViewer software, and ImageJ software was utilized for the quantitative analysis of positive staining area proportions.

Western blot

Total proteins were extracted from the right lung tissues using RIPA lysis buffer, and their concentrations were quantified using a BCA Protein Assay Kit. Equal amounts of protein (30 μg per lane) were subjected to sodium dodecyl sulfate-polyacrylamide gel electrophoresis (SDS-PAGE) and subsequently transferred onto polyvinylidene fluoride (PVDF) membranes. The membranes were blocked with QuickBlock™ Western Blocking Buffer for 15 min at room temperature.

Subsequently, the membranes were incubated overnight at 4 °C with the following primary antibodies: rabbit anti-TGF-β1 (1:1,000; Cat. No. AF1027, Affinity Biosciences), rabbit anti-Col-IV (1:1,000; Cat. No. AF0510, Affinity Biosciences), rabbit anti-p-Akt (1:1,000; Cat. No. AF0016, Affinity Biosciences), rabbit anti-Akt (1:1,000; Cat. No. AF6261, Affinity Biosciences), rabbit anti-TNF-α (1:500; Cat. No. 26162-1-AP, Proteintech), rabbit anti-fibronectin (1:2,000; Cat. No. 15613-1-AP, Proteintech), rabbit anti-GAPDH (1:5,000; Cat. No. 10494-1-AP, Proteintech), rabbit anti-p-PI3K (1:1,000; Cat. No. 4228, CST), and rabbit anti-PI3K (1:1,000; Cat. No. 4257, CST). After washing three times with Tris-buffered saline with Tween 20 (TBST), the membranes were incubated with an HRP-conjugated goat anti-rabbit IgG secondary antibody (1:5,000; Cat. No. 021042, EarthOx) for 1 h at room temperature. Finally, protein bands were visualized using an enhanced chemiluminescence (ECL) system, and their

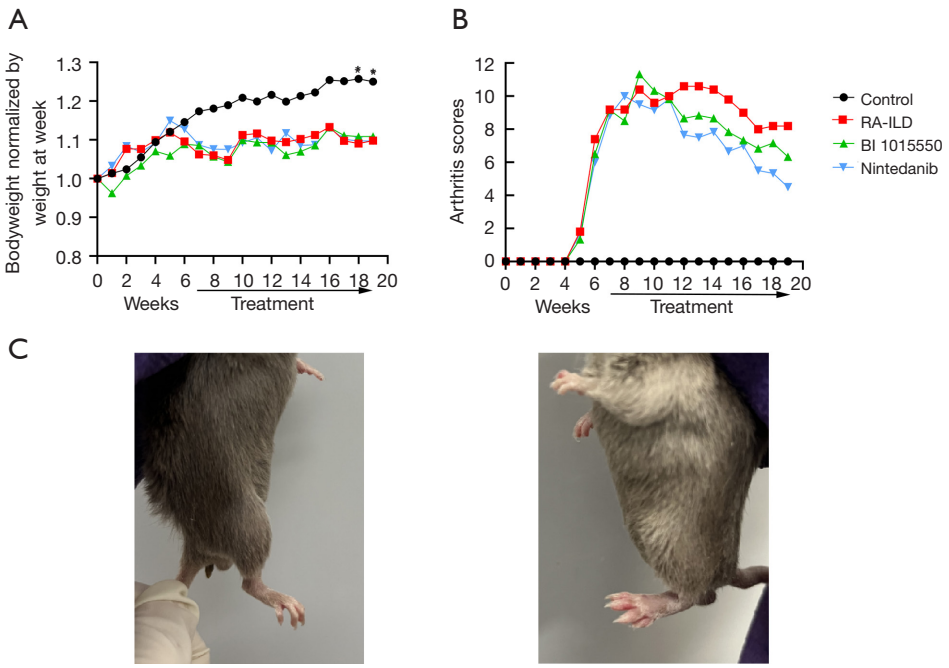

Figure 2 Effects of nerandomilast (BI 1015550) on body weight and arthritis severity in the RA-ILD mouse model. (A) Body weight of mice in each group (n≥3; *, P<0.05 *vs.* RA-ILD). (B) Visual arthritis scores of mice in each group (*vs.* RA-ILD). (C) Mouse joints: RA-ILD model group exhibited pronounced swelling and redness of the ankle and toe joints. BI 1015550 is the former investigational name for nerandomilast. RA-ILD, rheumatoid arthritis-associated interstitial lung disease.

intensities were quantified utilizing ImageJ software. GAPDH served as an internal control to normalize the relative expression of target proteins.

Statistical analysis

Statistical analysis was performed using GraphPad Prism 8.0 software, with data presented as the mean ± standard error of the mean (SEM). One-way analysis of variance (ANOVA) was performed for multi-group comparisons, while unpaired *t*-tests were applied for pairwise analysis. Data lacking normal distribution were analyzed using the nonparametric Kruskal-Wallis tests. A P<0.05 was considered statistically significant.

Results

Body weight and arthritis scores in experimental groups

From Weeks 0 to 19, body weight and visual arthritis scores were measured in all mice (*Figure 2*). Mice in the RA-ILD model, nerandomilast and nintedanib groups exhibited lower body weight than those in the control group, with no significant differences observed among the treatment and model groups (*Figure 2A*). Joint swelling was evidently noticed in RA-ILD model mice by Week 5, involving varying degrees of arthritis developing by Week 7. Treatment with either nerandomilast or nintedanib resulted in reduced visual arthritis scores compared to the RA-ILD model group, yet the differences were not statistically significant (*Figure 2B*). Besides, mice in the RA-ILD model group demonstrated noticeable swelling and redness in the ankle and toe joints (*Figure 2C*).

Nerandomilast reducing serum TNF-α levels in RA-ILD mice

Compared to the control group, serum TNF-α levels were significantly elevated in RA-ILD mice (P<0.05). Administration with nerandomilast or nintedanib considerably reduced serum TNF-α levels compared to the RA-ILD group (P<0.05; *Figure 3*).

Histopathological changes in lung tissue across groups

Lung tissue H&E staining demonstrated intact alveolar

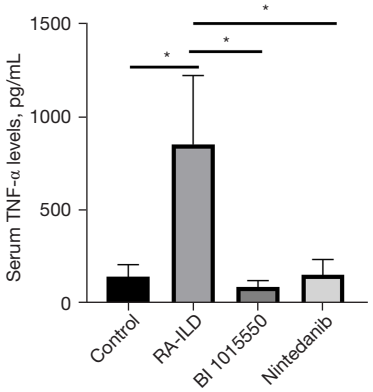

Figure 3 Serum TNF-α levels in experimental groups. Both nerandomilast (BI 1015550) and nintedanib treatment groups demonstrated significantly reduced TNF-α concentrations compared to the RA-ILD group (*, P<0.05; n≥3). BI 1015550 is the former investigational name for nerandomilast. RA-ILD, rheumatoid arthritis-associated interstitial lung disease; TNF-α, tumor necrosis factor-alpha.

septa without congestion, edema, or thickening in the control group, whereas the RA-ILD group exhibited pronounced alveolar septal edema, capillary congestion, thickening of the alveolar walls, and extensive infiltration of inflammatory cells. These pathological variations were markedly attenuated in the nerandomilast and nintedanib groups, as evidenced by reduced inflammatory cell infiltration and improved alveolar architecture. Further analysis uncovered that the pulmonary Szapiel scores were markedly lower in the nerandomilast and nintedanib groups than in the RA-ILD model group (P<0.05; *Figure 4A*,*4B*). Moreover, Masson's staining revealed only minimal blue-stained collagen deposition in the alveolar septa of the control group. In contrast, extensive blue-stained collagen deposition in the alveolar septa and alveolar collapse were detected in the RA-ILD group. These fibrotic changes were obviously reduced in the nerandomilast and nintedanib groups. Consistently, the modified Ashcroft scores of the two treatment groups were notably decreased compared to the RA-ILD group (P<0.05; *Figure 4A*,*4C*).

Histopathological evaluation of knee joint tissues

H&E staining revealed synovial hyperplasia and extensive inflammatory cell infiltration in the knee joints of RA-ILD mice (*Figure 5A*). These pathological alterations were attenuated in both the nerandomilast and nintedanib treatment groups. Notably, the synovitis score was remarkably reduced in the nerandomilast group compared to the RA-ILD group (P<0.05; *Figure 5B*). Moreover, Safranin O-Fast Green staining of knee joints in control mice demonstrated intact cartilage with bright red staining across the full thickness and well-preserved structural morphology, along with blue-green staining of subchondral bone. In contrast, cartilage from RA-ILD mice appeared weakly stained or unstained, indicating severe matrix degradation, structural disruption, and partial bone erosion. Degenerative lesions were effectively alleviated in both the nerandomilast and nintedanib groups. Cartilage damage scores were reduced in the treatment groups relative to the RA-ILD group, yet no statistical significance was observed (*Figure 5A*,*5C*). Additionally, immunohistochemical staining revealed evidently increased expression of TNF-α and MMP3 in the synovial tissues of RA-ILD mice compared to control mice. Treatment with nerandomilast or nintedanib distinctly decreased the positive staining areas of TNF-α and MMP3 relative to the RA-ILD group (P<0.05; *Figure 6*).

Effects of nerandomilast on pulmonary TNF-α, TGF-β1, and the PI3K/Akt signaling pathway

To further investigate the mechanisms underlying the attenuation of pulmonary fibrosis by nerandomilast and nintedanib in RA-ILD mice, Western blot analysis was conducted to evaluate the expression levels of TNF-α, TGF-β1, p-PI3K, total PI3K, p-Akt, and total Akt in lung tissues. The RA-ILD group exhibited significantly elevated levels of TNF-α, TGF-β1, p-PI3K, and p-Akt, whereas treatment with nerandomilast or nintedanib markedly reduced the expression of TNF-α and TGF-β1 (*Figure 7*). Additionally, the phosphorylation ratios of PI3K and Akt were markedly reduced in both treatment groups relative to

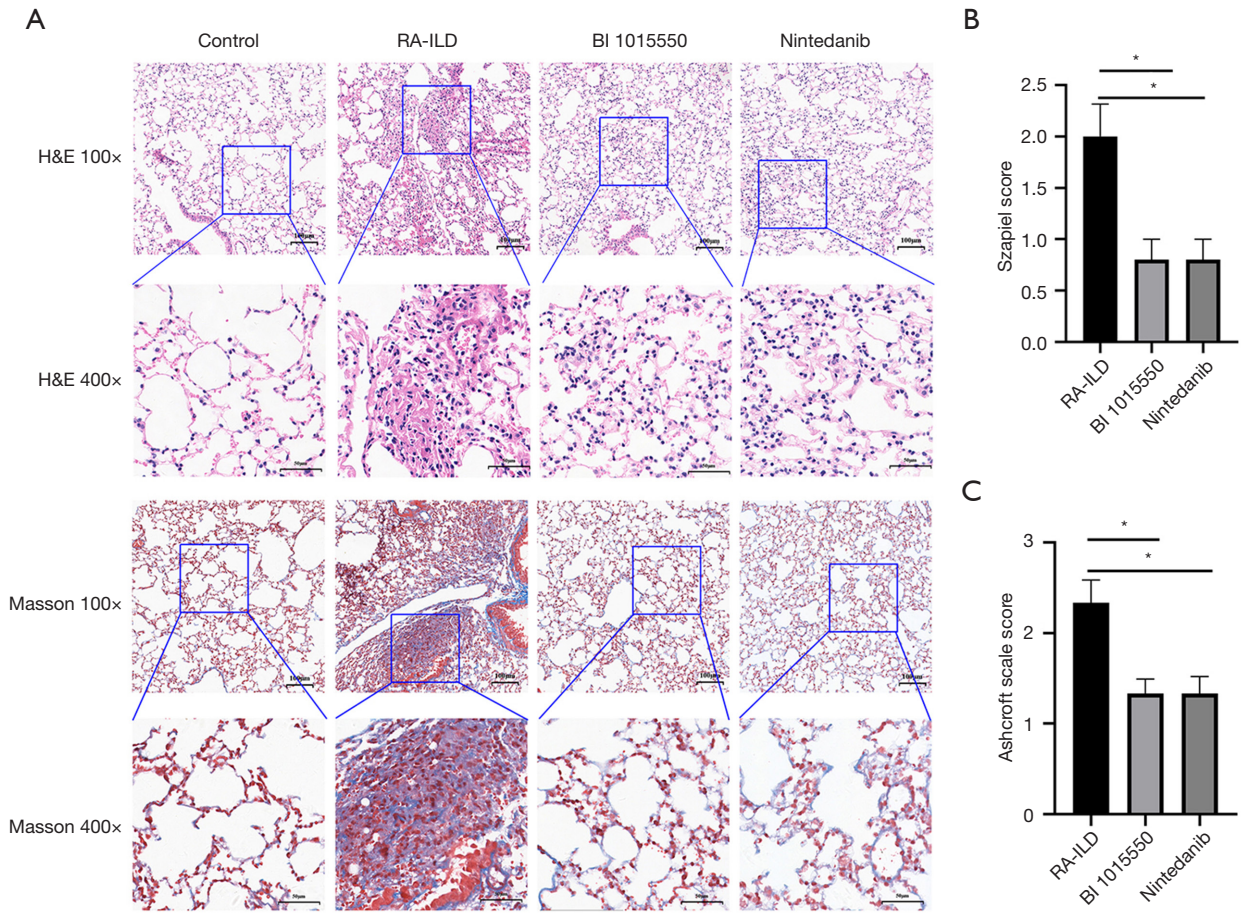

Figure 4 Nerandomilast (BI 1015550) and nintedanib alleviate lung inflammation and fibrosis in a collagen-induced RA-ILD mouse model. (A) H&E and Masson's staining of lung tissues from each group of mice; (B) pulmonary Szapiel scores; (C) modified Ashcroft scores of the lungs. n≥3. *, P<0.05. BI 1015550 is the former investigational name for nerandomilast. H&E, hematoxylin and eosin; RA-ILD, rheumatoid arthritis-associated interstitial lung disease.

the RA-ILD model group (*Figure 8*).

Effects of nerandomilast on ECM-related proteins and MMP3 expression in the lung

To evaluate the effects of nerandomilast and nintedanib on fibrosis-associated proteins, Western blotting was performed to detect the expression levels of ECM-related proteins, including collagen type IV (ColIV), fibronectin, and MMP3, in lung tissues from RA-ILD mice. The RA-ILD group exhibited significantly increased expression of MMP3, Col-IV, and fibronectin. In contrast, treatment with nerandomilast or nintedanib remarkably reduced the expression levels of these proteins (*Figure 9*).

Discussion

Pulmonary dysfunction resulting from RA-ILD remains a major cause of mortality among patients with RA (28). Despite the notable improvement in joint symptoms following biologic therapies, the mortality rate associated with RA-ILD continues to rise (29). Current studies have demonstrated immune-mediated pulmonary inflammation followed by fibrosis a key pathological process (30), rendering it necessarily important to further explore the therapeutic potential and underlying mechanisms of antifibrotic agents in RA-ILD.

In this study, CIA mice exhibited marked joint swelling. Histopathological examination of the knee joints revealed

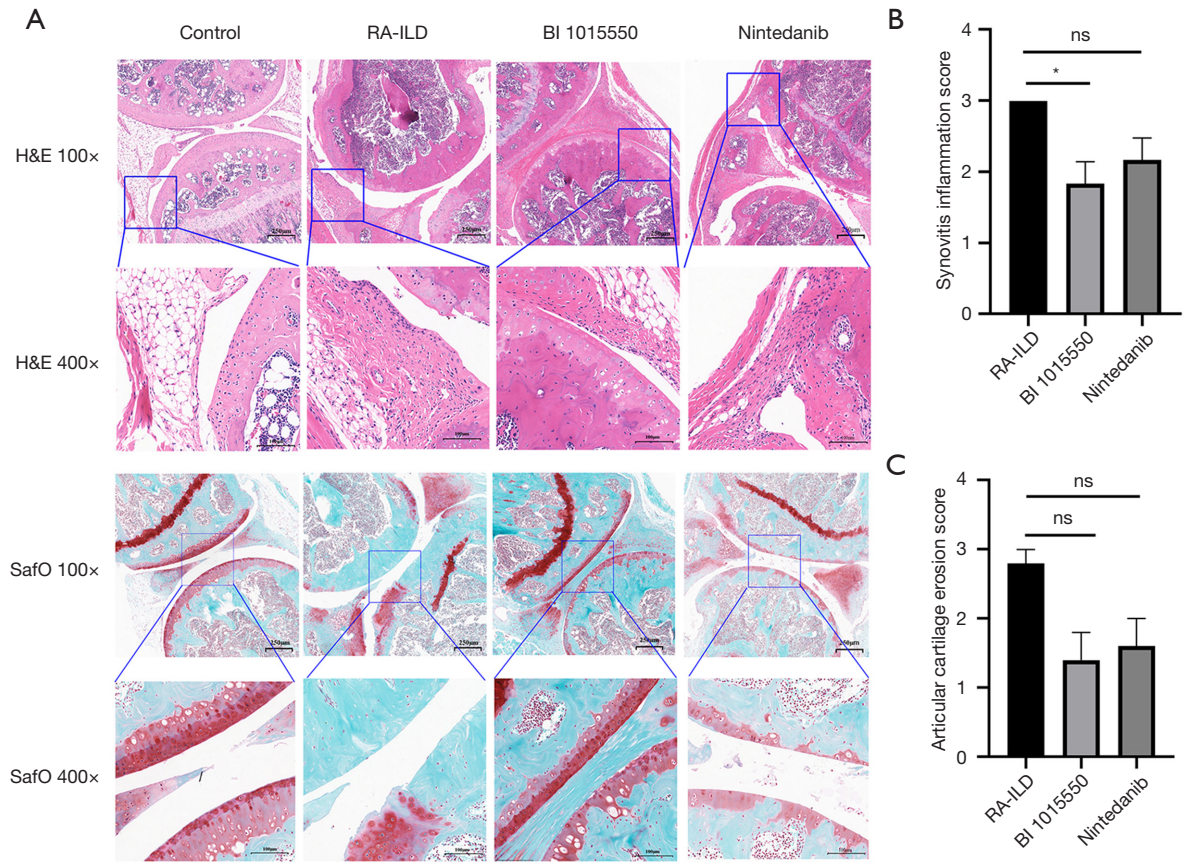

Figure 5 Effects of nerandomilast (BI 1015550) on histopathological changes in knee joints of RA-ILD mice. (A) H&E and SafO staining of knee joints from each group of mice. (B) Synovitis scores of knee joints, with the nerandomilast (BI 1015550) group showing lower scores than the RA-ILD group (n=3; *, P<0.05; ns, not significant). (C) Cartilage damage scores of knee joints. BI 1015550 is the former investigational name for nerandomilast. H&E, hematoxylin and eosin; RA-ILD, rheumatoid arthritis-associated interstitial lung disease; SafO, Safranin O-Fast Green.

prominent synovial hyperplasia and inflammatory cell infiltration, along with varying degrees of cartilage damage and bone erosion. Additionally, lung tissue analysis demonstrated alveolar wall thickening, inflammatory infiltration, and collagen deposition, which verified the successful establishment of the RA-ILD mouse model.

As a PDE4 inhibitor, nerandomilast exhibited a clear trend toward alleviating synovial inflammation and cartilage damage in the knee joints of RA mice. Apremilast, another PDE4 inhibitor, has been previously reported to improve arthritis scores and reduce bone erosion in RA mouse models, alongside the suppression of TNF-α production in human synovial cells (31). Consistent with these findings, nerandomilast markedly downregulated the expression of TNF-α and MMP3 in the knee joints of RA mice. Collectively, these results suggest that nerandomilast may alleviate arthritis by inhibiting TNF-α production in synovial tissue and reducing MMP3 secretion within the joints. Nevertheless, no significant intergroup differences were observed in either macroscopic arthritis scores or histological cartilage damage scores (P>0.05), which may be partially attributable to the limited sample size. Given the relatively slow progression of cartilage erosion, molecular improvements may precede detectable histological recovery during the course of joint lesion development. Furthermore, the microanatomical characteristics of the mouse knee joint precluded the isolation of pure synovial tissue for quantitative analyses by Western blotting or reverse transcription-quantitative polymerase chain reaction (RT-qPCR). Therefore, future studies incorporating larger cohorts and longer observation periods are required to further elucidate the therapeutic efficacy of nerandomilast in peripheral joint inflammation.

The present study prioritized the effects of nerandomilast

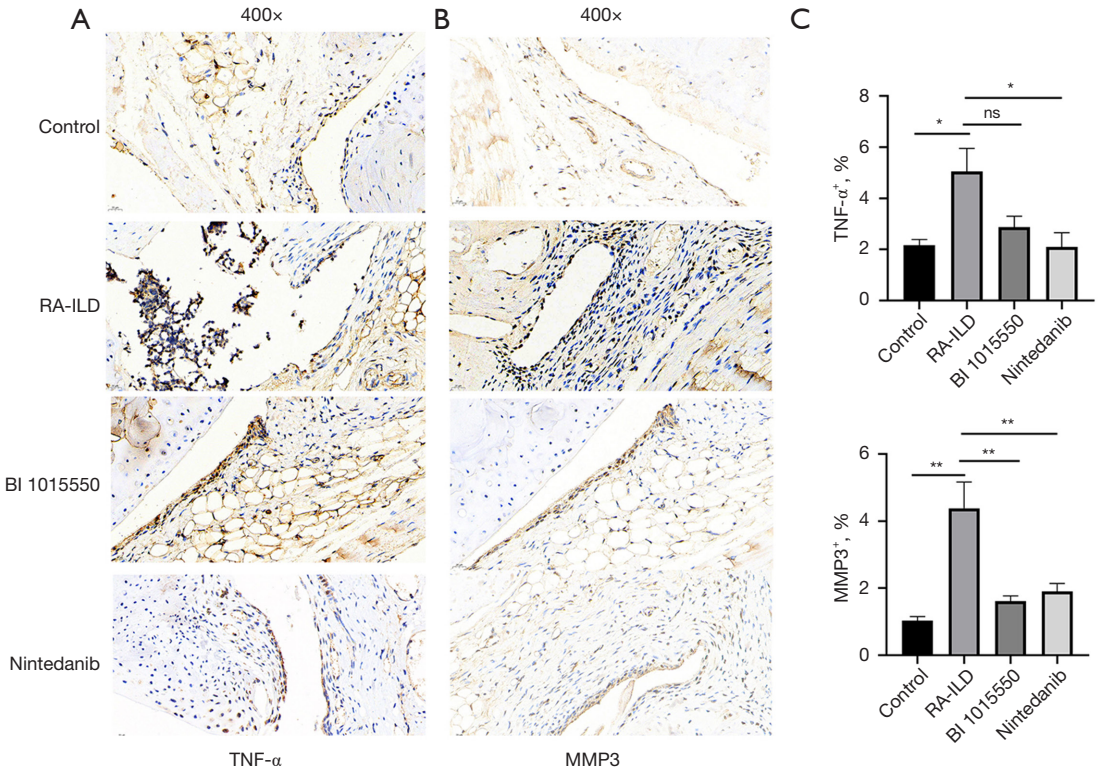

Figure 6 Nerandomilast (BI 1015550) suppresses TNF-α and MMP3 expression in synovial tissues of collagen-induced RA-ILD mice. (A) TNF-α immunohistochemical staining in mouse knee synovial tissue. (B) MMP3 immunohistochemical staining in mouse knee synovial tissue. (C) Percentage of TNF-α and MMP3 positive expression areas (n=3, *, P<0.05; **, P<0.01; ns, not significant). BI 1015550 is the former investigational name for nerandomilast. MMP3, matrix metalloproteinase-3; RA-ILD, rheumatoid arthritis-associated interstitial lung disease; TNF-α, tumor necrosis factor-alpha.

on the lungs of RA-ILD mice. Actually, the development of pulmonary fibrosis in RA-ILD involves a complex cytokine network (11), with TNF-α serving as a key pro-inflammatory mediator implicated in the pathogenesis of ILD (28). TNF-α plays a pivotal role in the pathogenesis of RA (32), and TNF-α inhibitors are also extensively used in RA treatment (33). Additionally, elevated TNF-α expression has been observed in the lungs and serum of RA-ILD rat model (34), as well as in the lungs of patients with idiopathic pulmonary fibrosis (IPF) (35). Notably, TNF-α inhibitors have been confirmed to attenuate bleomycin-induced pulmonary fibrosis in mice (36). As demonstrated previously, the PDE4 inhibitor rolipram suppresses TNF-α release from peripheral blood mononuclear cells (PBMCs) in RA-ILD patients (37), and nerandomilast inhibits lipopolysaccharide-induced TNF-α synthesis in human PBMCs (23). Herein, nerandomilast reduced TNF-α levels in both serum and lung tissue, while mitigating alveolar inflammation and fibrosis in RA-ILD mice. Collectively, these findings confirm that nerandomilast exerts potent anti-inflammatory effects by suppressing TNF-α release, thereby alleviating alveolitis and pulmonary fibrosis.

Current research indicates TGF-β as a key factor in the development of fibrosis across a wide range of tissues. TGF-β1 promotes the differentiation of human lung fibroblasts into myofibroblasts, resulting in excessive accumulation of ECM components, particularly collagen and fibronectin (38). TGF-β1 overexpression in rodent lungs has been demonstrated to induce severe pulmonary fibrosis (39). Besides, the profibrotic signaling of TGF-β is mediated through several intracellular pathways, including the PI3K/Akt pathway, enhancing fibrotic responses in lung tissues (40). The PI3K/Akt signaling pathway regulates multiple biological processes such as cell survival, proliferation, and metabolism (41). Mechanistically, this upstream signaling axis is mediated through direct

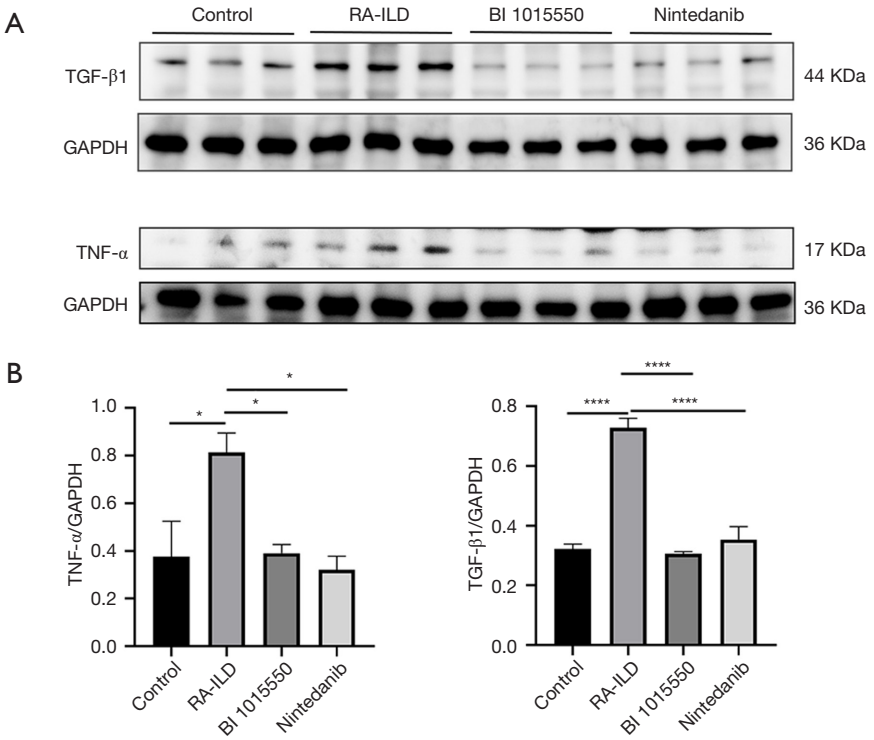

Figure 7 Effects of nerandomilast (BI 1015550) and nintedanib on pulmonary TNF-α and TGF-β1. (A) Western blot analysis of TNF-α and TGF-β1 protein expression in lung tissue. Both nerandomilast (BI 1015550) and nintedanib downregulated TNF-α levels and suppressed the TGF-β1 signaling pathway. (B) Relative expression levels of TNF-α and TGF-β1. *, P<0.05; ****, P<0.00001; n=3. BI 1015550 is the former investigational name for nerandomilast. GAPDH, glyceraldehyde-3-phosphate dehydrogenase; RA-ILD, rheumatoid arthritis-associated interstitial lung disease; TGF-β1, transforming growth factor-β1; TNF-α, tumor necrosis factor-alpha.

molecular interactions between TGF-β receptors and the PI3K complex. The regulatory subunit of PI3K, p85, constitutively associates with TGF-β receptor type II (TβRII), whereas its recruitment to TGF-β receptor type I (TβRI) is dynamically induced upon TGF-β1 stimulation. This ligand-dependent receptor assembly requires the intrinsic serine/threonine kinase activity of TβRI, thereby mediating non-canonical activation of the PI3K/Akt pathway (13,41). Activated Akt subsequently modulates downstream glycogen synthase kinase 3β (GSK-3β), mammalian target of rapamycin (mTOR), and forkhead box O3a (FOXO3a) signaling, collectively promoting fibroblast proliferation, apoptosis resistance, myofibroblast differentiation, and excessive ECM deposition. In parallel, activation of this signaling axis facilitates epithelial-mesenchymal transition (EMT), accelerates alveolar epithelial cell senescence, and promotes pro-fibrotic M2 macrophage polarization, thereby establishing a self-perpetuating feed-forward loop that drives the initiation and progression of pulmonary fibrosis (41-43). Inhibition of PI3K activity not only blocks Akt phosphorylation but also suppresses fibroblast proliferation, α-smooth muscle actin expression, and collagen production in the lungs (44). Notably, Akt2-deficient mice are protected against bleomycin-induced pulmonary fibrosis and inflammation (45). Moreover, upregulation of the PI3K/Akt pathway has been observed in RA-ILD (46). Herein, the expression levels of TGF-β1, p-PI3K, and p-Akt were observed to be remarkably elevated in the lung tissues of RA-ILD mice, whereas treatment with nerandomilast markedly reduced the expression of these proteins. Furthermore, nerandomilast significantly decreased the levels of ECM-related proteins, including Col IV and fibronectin. Collectively, these findings support the conclusion that nerandomilast mitigates pulmonary fibrosis in RA-ILD mice via regulation of the TGF-β1/PI3K/Akt signaling pathway.

Nintedanib, which is approved by the U.S. Food

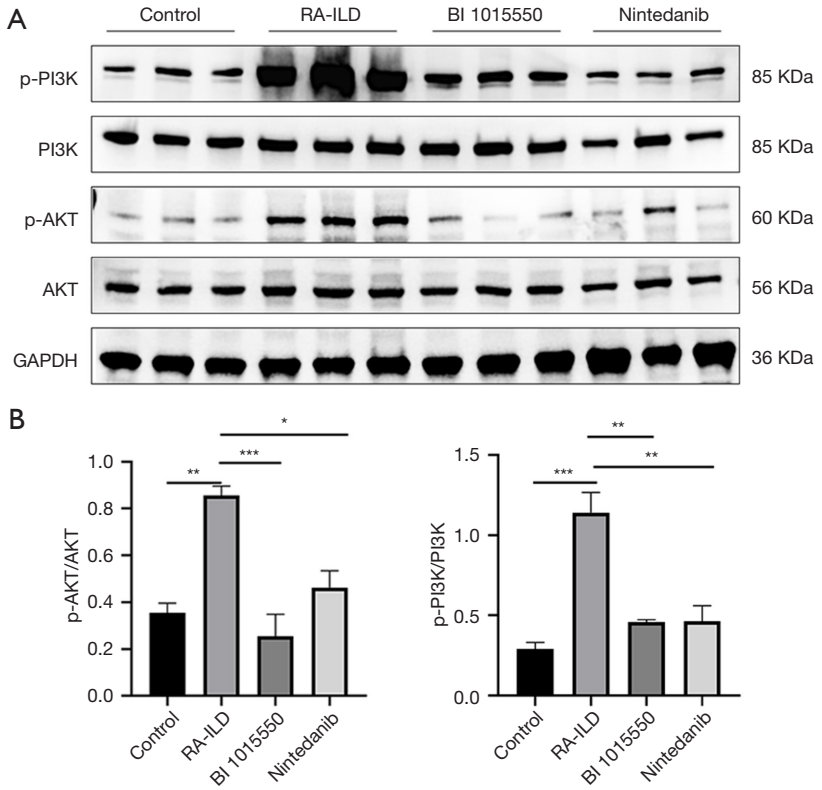

Figure 8 Effects of nerandomilast (BI 1015550) and nintedanib on the PI3K/Akt signaling pathway in the lung. (A) Western blot analysis of p-PI3K, total PI3K, p-Akt, and total Akt protein expression in lung tissue. (B) Relative expression levels of p-PI3K, PI3K, p-Akt, and Akt. *, P<0.01; **, P<0.001; ***, P<0.0001; n=3. BI 1015550 is the former investigational name for nerandomilast. GAPDH, glyceraldehyde-3-phosphate dehydrogenase; p-Akt, phospho-Akt; p-PI3K, phospho-PI3K; PI3K/Akt, phosphoinositide 3-kinase/protein kinase B; RA-ILD, rheumatoid arthritis-associated interstitial lung disease.

and Drug Administration (FDA) for treating IPF and progressive pulmonary fibrosis (PPF), is extensively used in clinical settings (47). Preclinical studies have demonstrated that nintedanib significantly attenuates pulmonary fibrosis in RA-ILD mouse models, while reducing joint swelling and arthritis scores (48,49). Furthermore, by downregulating the PI3K/Akt/mTOR signaling pathway, nintedanib mitigates bleomycin-induced pulmonary fibrosis (50). In the present study, nerandomilast exhibited anti-inflammatory and anti-fibrotic effects comparable to those of nintedanib. While both compounds demonstrate robust efficacy in halting fibrotic progression, they operate through distinct molecular mechanisms. Unlike nintedanib, which non-selectively blocks multi-tyrosine kinase receptors, nerandomilast is a novel, preferential phosphodiesterase 4B (PDE4B) inhibitor. This targeted inhibition precisely elevates intracellular cAMP levels, offering a distinct dual-action mechanism that simultaneously quenches upstream inflammatory cascades and suppresses downstream fibrotic remodeling (23,51).

Recent definitive evidence from global Phase III clinical trials—the FIBRONEER-IPF and FIBRONEER-ILD studies—has firmly established the clinical efficacy and superiority of nerandomilast in preventing lung function decline in patients with ILD, demonstrating a statistically significant stabilization of FVC over 52 weeks (52,53). Crucially, a dedicated subgroup analysis from the FIBRONEER-ILD trial specifically demonstrated that nerandomilast exhibits robust efficacy and favorable safety in patients with autoimmune disease-related PPF (54). Notably, nerandomilast provides a comparable preservation of lung function, whether administered as a standalone therapy or when added to background nintedanib (50,52). Furthermore, a major clinical advantage of nerandomilast lies in its

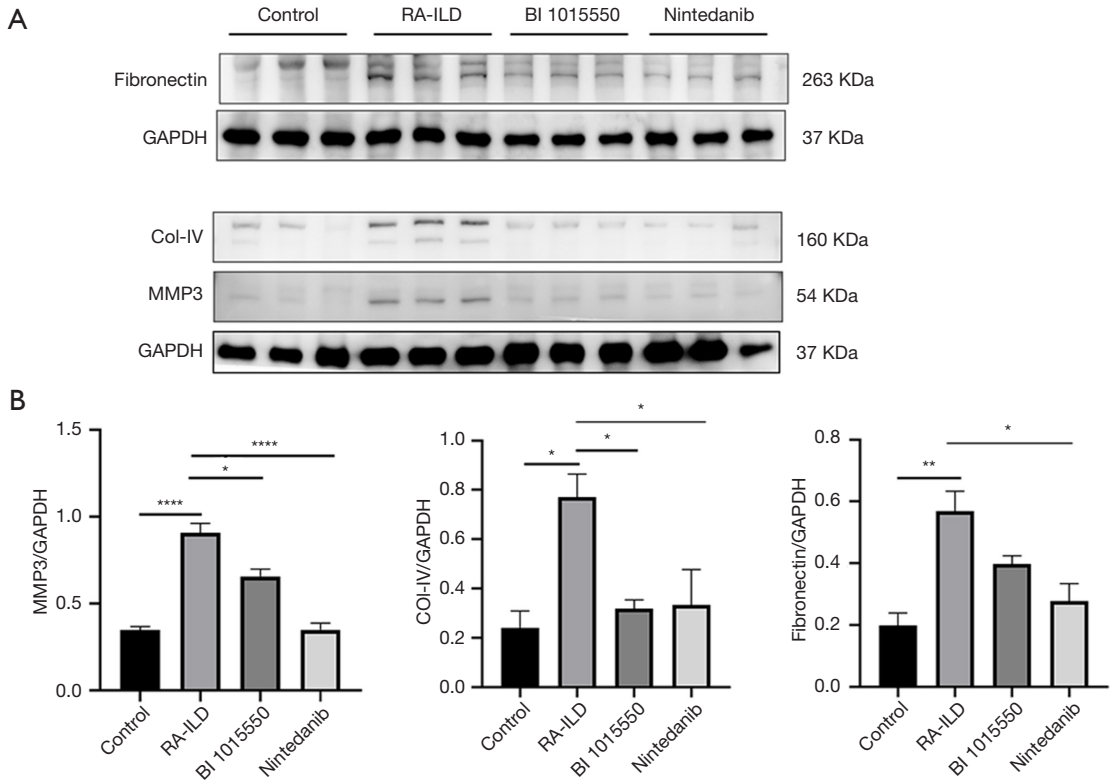

Figure 9 Effects of nerandomilast (BI 1015550) and nintedanib on ECM-related proteins in the lung. (A) Western blot analysis of Col-IV, fibronectin, and MMP3 protein expression in lung tissue. Both treatments downregulated Col-IV, fibronectin, and MMP3 levels. (B) Relative expression levels of Col-IV, fibronectin, and MMP3. *, P<0.01; **, P<0.001; ****, P<0.00001; n=3. BI 1015550 is the former investigational name for nerandomilast. Col-IV, collagen IV; ECM, extracellular matrix; GAPDH, glyceraldehyde-3-phosphate dehydrogenase; MMP3, matrix metalloproteinase-3; RA-ILD, rheumatoid arthritis-associated interstitial lung disease.

favorable gastrointestinal tolerability; unlike nintedanib, which is heavily limited by severe diarrhea, nerandomilast exhibits a significantly lower adverse-event-related discontinuation rate (55-57). This profile underscores its potential for flexible combination regimens as a prospective next-generation strategy. Collectively, these recent clinical and mechanistic milestones demonstrate that nerandomilast possesses both robust efficacy and an encouraging safety profile, suggesting substantial therapeutic value for the long-term management of RA-ILD.

The effects of nerandomilast on collagen-induced RA-ILD in the lungs and joints of mice were hereby investigated. As demonstrated by the results, nerandomilast attenuated pulmonary fibrosis by modulating the TGF-β1/PI3K/Akt signaling pathway, elucidating its potential anti-fibrotic mechanism. However, this study still has several limitations: (I) the sample size per experimental group was relatively small and unbalanced. To account for potential animal mortality during RA-ILD model establishment and gavage administration, the model and intervention groups were initially allocated more animals than the blank control group. Although key parameters demonstrated statistical significance, this limited and uneven sample size may have constrained statistical power. Future studies with larger, well-balanced cohorts are warranted to validate these findings; (II) it was conducted exclusively *in vivo* using a mouse model, involving no complementary *in vitro* cellular experiments; and (III) the therapeutic effects of nerandomilast on the lungs and joints of RA-ILD patients were not evaluated. Future studies should incorporate clinical samples to further validate these preclinical findings.

Conclusions

In conclusion, nerandomilast alleviates pulmonary

inflammation and fibrosis in RA-ILD mice by suppressing TNF-α release and downregulating the TGF-β1/PI3K/Akt signaling pathway. Overall, this study offers novel perspectives and potential therapeutic targets for the clinical application of nerandomilast in treating RA and its associated ILDs.

Acknowledgments

The authors gratefully acknowledge the contributions of Jie Zhang and Jia Liu in the experiments, and of Wenhan Huang in the writing of the manuscript.

Footnote

Reporting Checklist: The authors have completed the ARRIVE reporting checklist. Available at https://jtd.amegroups.com/article/view/10.21037/jtd-2026-1131/rc

Data Sharing Statement: Available at https://jtd.amegroups.com/article/view/10.21037/jtd-2026-1131/dss

Peer Review File: Available at https://jtd.amegroups.com/article/view/10.21037/jtd-2026-1131/prf

Funding: This study was supported by the Chongqing Clinical Research Center for Geriatric Diseases and the Chongqing Talents Program (No. cstc2024ycjh-bgzxm00061).

Conflicts of Interest: All authors have completed the ICMJE uniform disclosure form (available at https://jtd.amegroups.com/article/view/10.21037/jtd-2026-1131/coif). The authors have no conflicts of interest to declare.

Ethical Statement: The authors are accountable for all aspects of the work in ensuring that questions related to the accuracy or integrity of any part of the work are appropriately investigated and resolved. All animal experiments were performed under a project license (No. IAC-B2019011-P-01) granted by the Ethics Committee of Greentech, in compliance with institutional guidelines for the care and use of animals.

References

1. Smolen JS, Aletaha D, McInnes IB. Rheumatoid arthritis. Lancet 2016;388:2023-38.
2. Finckh A, Gilbert B, Hodkinson B, et al. Global epidemiology of rheumatoid arthritis. Nat Rev Rheumatol 2022;18:591-602.
3. Albrecht K, Strangfeld A, Marschall U, et al. Interstitial lung disease in rheumatoid arthritis: incidence, prevalence and related drug prescriptions between 2007 and 2020. RMD Open 2023;9:e002777.
4. Marigliano B, Soriano A, Margiotta D, et al. Lung involvement in connective tissue diseases: a comprehensive review and a focus on rheumatoid arthritis. Autoimmun Rev 2013;12:1076-84.
5. Chen J, Chen Y, Liu D, et al. Predictors of long-term prognosis in rheumatoid arthritis-related interstitial lung disease. Sci Rep 2022;12:9469.
6. Wang D, Zhang J, Lau J, et al. Mechanisms of lung disease development in rheumatoid arthritis. Nat Rev Rheumatol 2019;15:581-96.
7. Pugashetti JV, Lee JS. Overview of Rheumatoid Arthritis-Associated Interstitial Lung Disease and Its Treatment. Semin Respir Crit Care Med 2024;45:329-41.
8. Lee H, Lee SI, Kim HO. Recent Advances in Basic and Clinical Aspects of Rheumatoid Arthritis-associated Interstitial Lung Diseases. J Rheum Dis 2022;29:61-70.
9. Gabbiani G, Ryan GB, Majne G. Presence of modified fibroblasts in granulation tissue and their possible role in wound contraction. Experientia 1971;27:549-50.
10. Kim Y, Yang HI, Kim KS. Etiology and Pathogenesis of Rheumatoid Arthritis-Interstitial Lung Disease. Int J Mol Sci 2023;24:14509.
11. Huang C, Wu X, Wang S, et al. Combination of Salvia miltiorrhiza and ligustrazine attenuates bleomycin-induced pulmonary fibrosis in rats via modulating TNF-α and TGF-β. Chin Med 2018;13:36.
12. Györfi AH, Matei AE, Distler JHW. Targeting TGF-β signaling for the treatment of fibrosis. Matrix Biol 2018;68.
13. Finnson KW, Almadani Y, Philip A. Non-canonical (non-SMAD2/3) TGF-β signaling in fibrosis: Mechanisms and targets. Semin Cell Dev Biol 2020;101:115-22.

14. Saxton RA, Sabatini DM. mTOR Signaling in Growth, Metabolism, and Disease. Cell 2017;168:960-76.
15. Boutouja F, Stiehm CM, Platta HW. mTOR: A Cellular Regulator Interface in Health and Disease. Cells 2019;8:18.
16. Cantley LC. The phosphoinositide 3-kinase pathway. Science 2002;296:1655-7.
17. Azevedo MF, Faucz FR, Bimpaki E, et al. Clinical and molecular genetics of the phosphodiesterases (PDEs). Endocr Rev 2014;35:195-233.
18. Castelino FV, Adegunsoye A. Potential of phosphodiesterase 4B inhibitors in the treatment of interstitial lung disease associated with autoimmune diseases. Clin Exp Rheumatol 2025;43:119-25.
19. Pan JB, Hou YH, Zhang GJ. Rolipram attenuates bleomycin A5-induced pulmonary fibrosis in rats. Respirology 2009;14:975-82.
20. Udalov S, Dumitrascu R, Pullamsetti SS, et al. Effects of phosphodiesterase 4 inhibition on bleomycin-induced pulmonary fibrosis in mice. BMC Pulm Med 2010;10:26.
21. Sisson TH, Christensen PJ, Muraki Y, et al. Phosphodiesterase 4 inhibition reduces lung fibrosis following targeted type II alveolar epithelial cell injury. Physiol Rep 2018;6:e13753.
22. Cortijo J, Iranzo A, Milara X, et al. Roflumilast, a phosphodiesterase 4 inhibitor, alleviates bleomycin-induced lung injury. Br J Pharmacol 2009;156:534-44.
23. Herrmann FE, Hesslinger C, Wollin L, et al. BI 1015550 is a PDE4B Inhibitor and a Clinical Drug Candidate for the Oral Treatment of Idiopathic Pulmonary Fibrosis. Front Pharmacol 2022;13:838449.
24. Chen Y, Li Z, Li H, et al. Apremilast Regulates the Teff/Treg Balance to Ameliorate Uveitis via PI3K/AKT/FoxO1 Signaling Pathway. Front Immunol 2020;11:581673.
25. Szapiel SV, Elson NA, Fulmer JD, et al. Bleomycin-induced interstitial pulmonary disease in the nude, athymic mouse. Am Rev Respir Dis 1979;120:893-9.
26. Hübner RH, Gitter W, El Mokhtari NE, et al. Standardized quantification of pulmonary fibrosis in histological samples. Biotechniques 2008;44:507-11.
27. Hayer S, Vervoordeldonk MJ, Denis MC, et al. 'sMASH' recommendations for standardised microscopic arthritis scoring of histological sections from inflammatory arthritis animal models, et al. Ann Rheum Dis 2021;80:714-26.
28. Cavagna L, Monti S, Grosso V, et al. The multifaceted aspects of interstitial lung disease in rheumatoid arthritis. Biomed Res Int 2013;2013:759760.
29. Olson AL, Swigris JJ, Sprunger DB, et al. Rheumatoid arthritis-interstitial lung disease-associated mortality. Am J Respir Crit Care Med 2011;183:372-8.
30. Spagnolo P, Distler O, Ryerson CJ, et al. Mechanisms of progressive fibrosis in connective tissue disease (CTD)-associated interstitial lung diseases (ILDs). Ann Rheum Dis 2021;80:143-50.
31. McCann FE, Palfreeman AC, Andrews M, et al. Apremilast, a novel PDE4 inhibitor, inhibits spontaneous production of tumour necrosis factor-alpha from human rheumatoid synovial cells and ameliorates experimental arthritis. Arthritis Res Ther 2010;12:R107.
32. Okazaki H, Lin Q, Nishikawa K, et al. TNFα but not IL-17 is critical in the pathogenesis of rheumatoid arthritis spontaneously occurring in a unique FcγRIIB-deficient mouse model. Mod Rheumatol 2014;24:931-8.
33. Ma X, Xu S. TNF inhibitor therapy for rheumatoid arthritis. Biomed Rep 2013;1:177-84.
34. Yang G, Lyu L, Wang X, et al. Systemic treatment with resveratrol alleviates adjuvant arthritis-interstitial lung disease in rats via modulation of JAK/STAT/RANKL signaling pathway. Pulm Pharmacol Ther 2019;56:69-74.
35. Matsuhira T, Nishiyama O, Tabata Y, et al. A novel phosphodiesterase 4 inhibitor, AA6216, reduces macrophage activity and fibrosis in the lung. Eur J Pharmacol 2020;885:173508.
36. Altintas N, Erboga M, Aktas C, et al. Protective Effect of Infliximab, a Tumor Necrosis Factor-Alfa Inhibitor, on Bleomycin-Induced Lung Fibrosis in Rats. Inflammation 2016;39:65-78.
37. Song N, Liu AJ, Gao XF, et al. Effect of selective phosphodiesterase 4 inhibitors on nuclear factor kappa B, tumor necrosis factor-α and interleukin-8 expression in peripheral blood mononuclear cells in rheumatoid arthritis with interstitial lung disease. Zhonghua Nei Ke Za Zhi 2013;52:829-32.
38. Willis BC, Borok Z. TGF-beta-induced EMT: mechanisms and implications for fibrotic lung disease. Am J Physiol Lung Cell Mol Physiol 2007;293:L525-34.
39. Sime PJ, Xing Z, Graham FL, et al. Adenovector-mediated gene transfer of active transforming growth factor-beta1 induces prolonged severe fibrosis in rat lung. J Clin Invest 1997;100:768-76.
40. Harb I, Ashour H, Rashed LA, et al. Nicorandil mitigates amiodarone-induced pulmonary toxicity and fibrosis in association with the inhibition of lung TGF-β1/PI3K/Akt1-p/mTOR axis in rats. Clin Exp Pharmacol Physiol 2023;50:96-106.
41. Zhang YE. Non-Smad Signaling Pathways of the TGF-β

Family. Cold Spring Harb Perspect Biol 2017;9:a022129.
42. Wang J, Hu K, Cai X, et al. Targeting PI3K/AKT signaling for treatment of idiopathic pulmonary fibrosis. Acta Pharm Sin B 2022;12:18-32.
43. Bhatt J, Ghigo A, Hirsch E. PI3K/Akt in IPF: untangling fibrosis and charting therapies. Front Immunol 2025;16:1549277.
44. Conte E, Fruciano M, Fagone E, et al. Inhibition of PI3K prevents the proliferation and differentiation of human lung fibroblasts into myofibroblasts: the role of class I P110 isoforms. PLoS One 2011;6:e24663.
45. Nie Y, Sun L, Wu Y, et al. AKT2 Regulates Pulmonary Inflammation and Fibrosis via Modulating Macrophage Activation. J Immunol 2017;198:4470-80.
46. Yang Z, Han R, Yin H, et al. Mechanism of Lycopodii herba for RA-ILD using integrated metabolomics and network pharmacology. Anal Biochem 2022;648:114679.
47. Gole S, Bankole A. Nintedanib. In: StatPearls. Treasure Island (FL): StatPearls Publishing; 2024.
48. Liu J, Xu L, Guan X, et al. Experimental study of the effects of pirfenidone and nintedanib on joint inflammation and pulmonary fibrosis in a rheumatoid arthritis-associated interstitial lung disease mouse model. J Thorac Dis 2024;16:7458-76.
49. Redente EF, Aguilar MA, Black BP, et al. Nintedanib reduces pulmonary fibrosis in a model of rheumatoid arthritis-associated interstitial lung disease. Am J Physiol Lung Cell Mol Physiol 2018;314:L998-L1009.
50. Pan L, Cheng Y, Yang W, et al. Nintedanib Ameliorates Bleomycin-Induced Pulmonary Fibrosis, Inflammation, Apoptosis, and Oxidative Stress by Modulating PI3K/Akt/mTOR Pathway in Mice. Inflammation 2023;46:1531-42.
51. Sgalla G, Simonetti J, Cortese S, et al. BI 1015550: an investigational phosphodiesterase 4B (PDE4B) inhibitor for lung function decline in idiopathic pulmonary fibrosis (IPF). Expert Opin Investig Drugs 2023;32:17-23.
52. Maher TM, Assassi S, Azuma A, et al. Nerandomilast in Patients with Progressive Pulmonary Fibrosis. N Engl J Med 2025;392:2203-14.
53. Richeldi L, Azuma A, Cottin V, et al. Nerandomilast in Patients with Idiopathic Pulmonary Fibrosis. N Engl J Med 2025;392:2193-202.
54. Hoffmann-Vold AM, Assassi S, Cottin V, et al. Efficacy and safety of nerandomilast in patients with autoimmune disease-related progressive pulmonary fibrosis in the FIBRONEER-ILD trial. Ann Rheum Dis 2026;S0003-4967(26)00214-1.
55. Flaherty KR, Wells AU, Cottin V, et al. Nintedanib in Progressive Fibrosing Interstitial Lung Diseases. N Engl J Med 2019;381:1718-27.
56. Oldham JM, Azuma A, Kreuter M, et al. Nerandomilast in idiopathic pulmonary fibrosis: data from the whole follow-up period of the FIBRONEER-IPF trial. Am J Respir Crit Care Med 2026;212:972-80.
57. Wijsenbeek MS, Assassi S, Azuma A, et al. Nerandomilast in progressive pulmonary fibrosis: data from the whole follow-up period of the FIBRONEER-ILD trial. Eur Respir J 2026;68:2501899.

Cite this article as: Wang X, Liu X, Zhong X, Tang L. Nerandomilast (BI 1015550) attenuating pulmonary fibrosis in a mouse model of rheumatoid arthritis-associated interstitial lung disease by modulating the TGF-β1/PI3K/Akt signaling pathway. J Thorac Dis 2026;18(8):912. doi: 10.21037/jtd-2026-1131